

Mixed Elastic Modeling of Multilayer Composite Plates by Using Dimension Reduction Approach

M.J. Khoshgoftar^{a,*}, M. Shaban^b

^aMechanical Engineering Department, Arak University, Arak, Iran.

^bMechanical Engineering Department, Bu-Ali Sina University, Hamadan, Iran.

Article info

Article history:

Received 03 September 2018

Received in revised form

11 March 2019

Accepted 12 March 2019

Keywords:

Mixed variational formulation

Hellinger-Reissner principal

Linear elastic

Laminated plate

Elastic analysis

Abstract

In this paper, a mixed modeling approach for orthotropic laminated plates is developed. By adopting Hellinger-Reissner functional and dimension reduction method along the thickness, the governing equations were derived. By considering other theories i.e. classical plate theory, first order shear deformation theory and elasticity theory, the advantages of the current work are illustrated with some numerical results. Excellent agreements were observed by comparing the obtained results with three-dimensional elasticity theory for laminated thick plates. In the presented method, shear correction factor was not required for considering shear strain components. Furthermore, finite element simulation was implemented in Abaqus software by using two-dimensional shell elements and compared with obtained results. It is seen that although finite element model predicts good results for displacement field but it cannot provide any suitable results in thickness direction.

Nomenclature

\mathbf{D}	Elastic tensor	ν	Poisson ratio
E	Elastic modulus	h	Thickness
Ω	Plate domain	B	Second plate dimension
\mathbf{s}	Displacement vector	$\boldsymbol{\sigma}$	Stress tensor
\mathbf{f}	Force vector	\mathbf{n}	Normal vector
a	First plate dimension	G	Shear modulus

1. Introduction

In the recent decades, several plate and shell theories have been proposed in the literature for predicting mechanical behavior of laminated panels. Classical plate theory (CPT) and first order shear deformation theory (FSDT) are two famous theories widely used by other researchers. Based on Kirchhoff-Love assumptions, classical theory neglects the shear deformation, so it leads to inaccurate results. The principal assumption in CPT is that normal lines to the mid-plane be-

fore deformation remain straight and normal to the plane after deformation. On the other hand, in FSDT approach, the shear deformation components are not neglected and are considered to be constant along the thickness. However, this theory gives satisfactory results for practical cases and it is need to adopt the shear correction factor for achieving more accurate results. Determining shear correction factor is not always easy for all cases and the well-known value $5/6$ is suitable only for homogenous plates.

The earlier investigations on the analysis of com-

*Corresponding author: M.J. Khoshgoftar (Assistant Professor)

E-mail address: mj.khoshgoftar@gmail.com

<http://dx.doi.org/10.22084/jrstan.2019.17217.1063>

ISSN: 2588-2597

posite laminated plates with different theories can be found in the good review paper of Khandan et al. [1]. Khandan et al. [1] focused on the accuracy and efficiency of various theories in predicting transverse shear strains and stresses. It was shown that in contrast to higher-order shear deformation theory, common CPT and FSDT are unable to obtain reasonable shear stress. The higher-order shear theories are based on nonlinear stress variation through the thickness and have been advised by numerous researchers to avoid using shear correction factors. However, some of these models do not satisfy the continuity conditions of transverse shear stresses at the layer interfaces for composite laminates. As an example, Reddy and Kim [2] proposed a general third order theory for functionally graded plates by considering microstructure dependent length scale parameter and showed that the third order shear deformation theory (TSDT), FSDT and CPT can be obtained as special cases of the general third order theory.

On the other hand, the elasticity models obtain exact representation without any simplifications but require heavy computational processing. Furthermore, these models are impractical for engineering applications because the number of variables in these models directly depend on the number of layers. One of the best investigations was done by Pagano [3] for rectangular laminated plates with pinned edges based on three-dimensional elasticity theory. He compared the elasticity solution with classical laminated plate theory and showed that the accuracy of CPT depends upon material properties, lamination geometry, and span to depth ratio. Moreover, CPT shows slower convergence for layered plates compared with exact solution.

The mixed variational approach is a powerful tool based on the variational principles. This model was firstly developed by Hellinger and then was improved by Khandan et al. [1]. Reissner proposed a mixed formulation as a tool to variationally derive the governing equilibrium and constitutive equations in terms of independent variables [4]. The derivation of two-dimensional models for bending and stretching of thin three-dimensional elastic plates using variational method was provided by Alessandrini et al. [5]. Wu and Li [6] investigated bending behavior of simply supported multilayered composite laminates and FGM plates, using Reissner mixed variational theorem and principle of virtual displacement based on finite layer method. In other work, Wu et al. [7] developed Reissner mixed variational theorem based on TSDT and studied static analysis of simply supported multilayered composite and FGM plates under mechanical loads. Carrera [8] used both mixed and classical theories to study the global and local responses of multilayered orthotropic plates, and concluded that the Reissner mixed variational theorem based theories are superior to the principle of virtual displacement-based ones. A generalized unified formulation (GUF) was devel-

oped by Demasi to investigate the Reissner mixed variational theorem-based theories, including mixed first-order and higher-order shear deformation theory, zig-zag, layerwise theories [9-13].

There are many publications which used dimension reduction method for boundary value problems. According to Vogelius and Babuska [14], this method is able to adopt and solve a $(n + 1)$ dimensional boundary value problem by replacing them with system of equations in n dimensional space by considering linear combination of functions. Liu [15] used dimensional reduction method for elasticity plate on an unbounded domain. He estimated error between exact solution and reduced solution and showed the capability of this method for analysis of plates. Various numerical investigations used reduction approach based on discretization methods such as finite element, finite difference, etc. For instance, by adopting a mixed enhanced variational formulation and FSDT, Auricchio and Sacco [16] presented a finite element method for laminated composite plates with an accurate evaluation of shear correction factor. Another mixed model based on FSDT was presented by Daghia et al. [17] by implementing a new quadratic four-node finite element from a hybrid stress formulation. Moleiro et al [18] developed a layerwise finite element model in a mixed least square formulation for static analysis of multilayered composite plates and showed that proposed method has very good agreement with three-dimensional solution and is insensitive to shear locking. In other article, Auricchio et al. [19] introduced new planer linear elastic beams based on Hellinger-Reissner principle. It was shown that the shear correction factor is considered naturally from the variational derivation and their model can capture the local effects produced by boundary constrains and load distribution. Additionally, they applied their proposed model for three-dimensional beams and derived beam model using variational dimension reduction approach [20].

In the work done by D'Ottavio [21], the multilayered composite panel was divided into subdivision layers and for each sublayer, the formulation was independently developed. Finally, the sublayers were assembled and layerwise conditions were introduced. There were several investigations which used plate and shell theories for nano/micro-structures by modifying the stress tensor. Instantly, Arefi et al. [22] used extended FSDT by considering modified couple stress theory to predict the vibration behavior of three-layered nano plates rested on Pasternak foundation. In other work [23], they used sinusoidal shear deformation theory to study the bending of a sandwich microbeam with two piezoelectric micro face-sheets. Ribeiro et al. [24], in their good work, examined the accuracy and limita-

tions of Carrera's Unified Formulation by comparing the results with experimental tests. They also developed a FORTRAN user subroutine for finite element model and compared the obtained numerical results with experimental ones.

In this paper, a new elastic analysis method based on dimension reduction approach and Hellinger-Reissner principle is presented. At the first, shape functions obtained with arbitrary coefficients were adopted along the thickness of plate for both displacement and stress field. Then governing partial differential equations of plate were derived by using the Hellinger-Reissner principle. After that, results of the presented model were compared with other plate theories. The obtained results were compared with finite element method and the capability of the presented approach was discussed. The main goal of this paper is deriving a plate theory that provides an accurate description for stress and displacement field. This theory can be used for both thin and moderator thick plates. Besides, thick, inhomogeneous, non-linear, and functionally graded materials could be formulated with this approach. According to implemented Hellinger-Reissner principle, the stress field is independent of displacement field. The presented theory does not need any correction factor and will lead to an accurate in-plane and out-of-plane stress and displacement distributions.

2. Formulation

Consider an elastic plate with initially flat surface having thickness h , length a , and width b . The plate is made of orthotropic material with piecewise smooth boundaries and is subjected to bending loads. Based on Hellinger-Reissner variational principle [19], for an elastic rectangular plate, according to divergence operator the following relation can be written as

$$\begin{aligned} \delta J_{HR} = & \int_{\Omega} \delta \mathbf{s} \cdot \nabla \cdot \boldsymbol{\sigma} d\Omega + \int_{\Omega} \nabla \cdot \delta \boldsymbol{\sigma} \cdot \mathbf{s} d\Omega \\ & + \int_{\Omega} \delta \boldsymbol{\sigma} : \mathbf{D}^{-1} : \boldsymbol{\sigma} d\Omega + \int_{\Omega} \delta \mathbf{s} \cdot \mathbf{f} d\Omega \\ & - \int_{\partial\Omega_s} \delta \boldsymbol{\sigma} \cdot \mathbf{n} \cdot \bar{\mathbf{s}} d\Omega_s = 0 \end{aligned} \quad (1)$$

where \mathbf{s} is displacement field vector and $\boldsymbol{\sigma}$ is the stress field matrix. The problem domain Ω is defined in equation (2) and is shown in Fig. 1 and Ω_s is boundary domain.

$$\Omega = \left\{ (x, y, z) \in \mathcal{R}^3 \mid z \in \left(-\frac{h}{2}, \frac{h}{2} \right), \right. \\ \left. (x, y) \in A \subset \mathcal{R}^2 \right\} \quad (2)$$

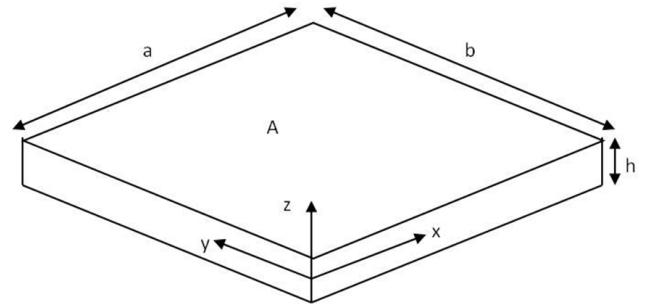


Fig. 1. Problem domain, coordinate system and dimension.

$\bar{\mathbf{s}}$ is the prescribed boundary displacement that was applied to $\partial\Omega_s$ that is defined in equation (3) and \mathbf{f} is a body force density.

$$\mathbf{s} = \bar{\mathbf{s}} \quad \text{on} \quad \Omega = \partial\Omega_s \quad (3)$$

\mathbf{D} is a sixth order linear and elastic stiffness tensor that depends on the material parameters. For orthotropic material, \mathbf{D} is as follows [25]:

$$\mathbf{D}^{-1} = \begin{bmatrix} \frac{1}{E_x} & -\frac{\nu_{yx}}{E_x} & -\frac{\nu_{zx}}{E_x} & 0 & 0 & 0 \\ -\frac{\nu_{xy}}{E_y} & \frac{1}{E_y} & -\frac{\nu_{zy}}{E_z} & 0 & 0 & 0 \\ -\frac{\nu_{xz}}{E_x} & -\frac{\nu_{yz}}{E_y} & \frac{1}{E_z} & 0 & 0 & 0 \\ 0 & 0 & 0 & \frac{1}{G_{xy}} & 0 & 0 \\ 0 & 0 & 0 & 0 & \frac{1}{G_{xz}} & 0 \\ 0 & 0 & 0 & 0 & 0 & \frac{1}{G_{yz}} \end{bmatrix} \quad (4)$$

where E_i , G_{ij} and ν_{ij} denote elastic modulus, shear modulus, and Poisson's ratio, respectively. ($i = x, y, z$). At the first step, the dimension of problem was reduced with a combination of cross-section shape functions that weighted with arbitrary coefficient functions that defined in equation (5).

$$\boldsymbol{\gamma}(x, y, z) = \mathbf{r}_\gamma(z) \hat{\boldsymbol{\gamma}}(x, y) \quad (5)$$

Adopting Eq. (5) in displacement field is shown in Eq. (6) where u , ν , and w are displacement components along the x , y , and z directions.

$$\begin{aligned} \mathbf{s} &= \begin{Bmatrix} u(x, y, z) \\ \nu(x, y, z) \\ w(x, y, z) \end{Bmatrix} \\ &\approx \begin{bmatrix} \mathbf{r}_u^T(z) & \mathbf{0} & \mathbf{0} \\ \mathbf{0} & \mathbf{r}_\nu^T(z) & \mathbf{0} \\ \mathbf{0} & \mathbf{0} & \mathbf{r}_w^T(z) \end{bmatrix} \begin{Bmatrix} \hat{\mathbf{u}}(x, y) \\ \hat{\boldsymbol{\nu}}(x, y) \\ \hat{\mathbf{w}}(x, y) \end{Bmatrix} \\ &= \mathbf{r}_s \hat{\mathbf{s}} \end{aligned} \quad (6)$$

Also the dimension reduction for stress field is applied in Eq. (7).

$$\boldsymbol{\sigma} = \begin{Bmatrix} \sigma_x(x, y, z) \\ \sigma_y(x, y, z) \\ \sigma_z(x, y, z) \\ \tau_{xy}(x, y, z) \\ \tau_{xz}(x, y, z) \\ \tau_{yz}(x, y, z) \end{Bmatrix} \approx \begin{bmatrix} \mathbf{r}_{\sigma_x}^T(z) & \mathbf{0} & \mathbf{0} & \mathbf{0} & \mathbf{0} & \mathbf{0} \\ \mathbf{0} & \mathbf{r}_{\sigma_y}^T(z) & \mathbf{0} & \mathbf{0} & \mathbf{0} & \mathbf{0} \\ \mathbf{0} & \mathbf{0} & \mathbf{r}_{\sigma_z}^T(z) & \mathbf{0} & \mathbf{0} & \mathbf{0} \\ \mathbf{0} & \mathbf{0} & \mathbf{0} & \mathbf{r}_{\tau_{xy}}^T(z) & \mathbf{0} & \mathbf{0} \\ \mathbf{0} & \mathbf{0} & \mathbf{0} & \mathbf{0} & \mathbf{r}_{\tau_{xz}}^T(z) & \mathbf{0} \\ \mathbf{0} & \mathbf{0} & \mathbf{0} & \mathbf{0} & \mathbf{0} & \mathbf{r}_{\tau_{yz}}^T(z) \end{bmatrix} \begin{Bmatrix} \hat{\boldsymbol{\sigma}}_x(x, y) \\ \hat{\boldsymbol{\sigma}}_y(x, y) \\ \hat{\boldsymbol{\sigma}}_z(x, y) \\ \hat{\boldsymbol{\tau}}_{xy}(x, y) \\ \hat{\boldsymbol{\tau}}_{xz}(x, y) \\ \hat{\boldsymbol{\tau}}_{yz}(x, y) \end{Bmatrix} = \mathbf{r}_\sigma \hat{\boldsymbol{\sigma}} \quad (7)$$

So, according to definition of displacement and stress field, the principle of variation is defined in Eq. (8) as follows:

$$\begin{aligned} \delta \mathbf{s} &= \mathbf{r}_s \delta \hat{\mathbf{s}} \\ \delta \boldsymbol{\sigma} &= \mathbf{r}_\sigma \delta \hat{\boldsymbol{\sigma}} \end{aligned} \quad (8)$$

In Eq. (1), ∇ is gradient operator. The divergence of stress and normal traction field is defined in Eqs. (9) and (10).

$$\nabla \cdot \boldsymbol{\sigma} = \left(\frac{\partial}{\partial x} \mathbf{E}_1 + \frac{\partial}{\partial y} \mathbf{E}_2 + \frac{\partial}{\partial z} \mathbf{E}_3 \right) \boldsymbol{\sigma} \quad (9)$$

$$\boldsymbol{\sigma} \cdot \mathbf{n} = (n_x \mathbf{E}_1 + n_y \mathbf{E}_2 + n_z \mathbf{E}_3) \boldsymbol{\sigma} \quad (10)$$

where $E_i (i = 1, 2, 3)$ is defined in Eq. (11).

$$\begin{aligned} \mathbf{E}_1 &= \begin{bmatrix} 1 & 0 & 0 & 0 & 0 & 0 \\ 0 & 0 & 0 & 1 & 0 & 0 \\ 0 & 0 & 0 & 0 & 1 & 0 \end{bmatrix} \\ \mathbf{E}_2 &= \begin{bmatrix} 0 & 0 & 0 & 1 & 0 & 0 \\ 0 & 1 & 0 & 0 & 0 & 0 \\ 0 & 0 & 0 & 0 & 0 & 1 \end{bmatrix} \\ \mathbf{E}_3 &= \begin{bmatrix} 0 & 0 & 0 & 0 & 1 & 0 \\ 0 & 0 & 0 & 0 & 0 & 1 \\ 0 & 0 & 1 & 0 & 0 & 0 \end{bmatrix} \end{aligned} \quad (11)$$

By substituting Eqs. (8), (9) and (10) into Eq. (1), the following relation is obtained as below:

$$\begin{aligned} \delta J_{HR} &= \int_{\Omega} [\mathbf{r}_s \delta \hat{\mathbf{s}}]^T \left[\left(\frac{\partial}{\partial x} \mathbf{E}_1 + \frac{\partial}{\partial y} \mathbf{E}_2 + \frac{\partial}{\partial z} \mathbf{E}_3 \right) \mathbf{r}_\sigma \hat{\boldsymbol{\sigma}} \right] d\Omega \\ &+ \int_{\Omega} \left[\left(\frac{\partial}{\partial x} \mathbf{E}_1 + \frac{\partial}{\partial y} \mathbf{E}_2 + \frac{\partial}{\partial z} \mathbf{E}_3 \right) \mathbf{r}_\sigma \delta \hat{\boldsymbol{\sigma}} \right]^T [\mathbf{r}_s \hat{\mathbf{s}}] d\Omega \\ &+ \int_{\Omega} [\mathbf{r}_\sigma \delta \hat{\boldsymbol{\sigma}}]^T \mathbf{D}^{-1} \mathbf{r}_\sigma \delta \hat{\boldsymbol{\sigma}} d\Omega + \int_{\Omega} [\mathbf{r}_s \delta \hat{\mathbf{s}}]^T \mathbf{f} d\Omega \\ &- \int_{\partial\Omega_s} [(n_x \mathbf{E}_1 + n_y \mathbf{E}_2 + n_z \mathbf{E}_3) \mathbf{r}_\sigma \delta \hat{\boldsymbol{\sigma}}]^T \bar{\mathbf{s}} d\Omega_s = 0 \quad (12) \end{aligned}$$

By expanding the products and assuming natural displacement condition along the thickness, Eq. (12) can

be rewritten as follows:

$$\begin{aligned} &\int_{\Omega} [\delta \hat{\mathbf{s}}^T \mathbf{r}_s^T \mathbf{E}_3 \mathbf{r}_{\sigma_z} \hat{\boldsymbol{\sigma}} + \delta \hat{\mathbf{s}}^T \mathbf{r}_s^T \mathbf{E}_1 \mathbf{r}_{\sigma_x} \hat{\boldsymbol{\sigma}} + \delta \hat{\mathbf{s}}^T \mathbf{r}_s^T \mathbf{E}_2 \mathbf{r}_{\sigma_y} \hat{\boldsymbol{\sigma}} \\ &+ \delta \hat{\boldsymbol{\sigma}}^T \mathbf{r}_{\sigma_z}^T \mathbf{E}_3^T \mathbf{r}_s \hat{\mathbf{s}} + \delta \hat{\boldsymbol{\sigma}}^T \mathbf{r}_{\sigma_x}^T \mathbf{E}_1^T \mathbf{r}_s \hat{\mathbf{s}} + \delta \hat{\boldsymbol{\sigma}}^T \mathbf{r}_{\sigma_y}^T \mathbf{E}_2^T \mathbf{r}_s \hat{\mathbf{s}} \\ &+ \delta \hat{\boldsymbol{\sigma}}^T \mathbf{r}_{\sigma}^T \mathbf{D}^{-1} \mathbf{r}_\sigma \delta \hat{\boldsymbol{\sigma}} + \delta \hat{\mathbf{s}}^T \mathbf{r}_s^T \mathbf{f}] d\Omega \\ &- \int_{\partial\Omega_s} \delta \hat{\boldsymbol{\sigma}}^T \mathbf{r}_{\sigma}^T \mathbf{E}_3^T \bar{\mathbf{s}} d\Omega_s = 0 \end{aligned} \quad (13)$$

Recalling the problem domain in Eq. (14) and summarizing the Eq. (13) according to problem domain, Eq. (15) is obtained.

$$\Omega = t \times A, \quad t \left(-\frac{h}{2}, \frac{h}{2} \right) \subset \mathbb{R}, \quad A \subset \mathbb{R}^2 \quad (14)$$

$$\begin{aligned} &\int_A [\delta \hat{\mathbf{s}}^T \mathbf{H}_{s\sigma} \hat{\boldsymbol{\sigma}} + \delta \hat{\mathbf{s}}^T \mathbf{G}_{s\sigma}^x \hat{\boldsymbol{\sigma}} + \delta \hat{\mathbf{s}}^T \mathbf{G}_{s\sigma}^y \hat{\boldsymbol{\sigma}} \\ &+ \delta \hat{\boldsymbol{\sigma}}^T \mathbf{H}_{\sigma s} \hat{\mathbf{s}} + \delta \hat{\boldsymbol{\sigma}}^T \mathbf{G}_{\sigma s}^x \hat{\mathbf{s}} + \delta \hat{\boldsymbol{\sigma}}^T \mathbf{G}_{\sigma s}^y \hat{\mathbf{s}} + \delta \hat{\boldsymbol{\sigma}}^T \mathbf{H}_{\sigma\sigma} \hat{\boldsymbol{\sigma}} \\ &- \delta \hat{\mathbf{s}}^T \mathbf{F}] dA + \delta \hat{\boldsymbol{\sigma}}^T \bar{\mathbf{S}} = 0 \end{aligned} \quad (15)$$

where \mathbf{G} , \mathbf{H} , \mathbf{F} and $\bar{\mathbf{S}}$ is defined as follows:

$$\begin{aligned} \mathbf{H}_{s\sigma} &= \int_{-\frac{h}{2}}^{\frac{h}{2}} \mathbf{r}_s^T \mathbf{E}_3 \mathbf{r}_{\sigma_z} dz & \mathbf{H}_{\sigma s} &= \int_{-\frac{h}{2}}^{\frac{h}{2}} \mathbf{r}_{\sigma_z}^T \mathbf{E}_3^T \mathbf{r}_s dz \\ \mathbf{H}_{\sigma\sigma} &= \int_{-\frac{h}{2}}^{\frac{h}{2}} \mathbf{r}_{\sigma}^T \mathbf{D}^{-1} \mathbf{r}_{\sigma} dz & \mathbf{G}_{s\sigma}^x &= \int_{-\frac{h}{2}}^{\frac{h}{2}} \mathbf{r}_s^T \mathbf{E}_1 \mathbf{r}_{\sigma_x} dz \\ \mathbf{G}_{s\sigma}^y &= \int_{-\frac{h}{2}}^{\frac{h}{2}} \mathbf{r}_s^T \mathbf{E}_2 \mathbf{r}_{\sigma_y} dz & \mathbf{G}_{\sigma s}^x &= \int_{-\frac{h}{2}}^{\frac{h}{2}} \mathbf{r}_{\sigma_x}^T \mathbf{E}_1^T \mathbf{r}_s dz \end{aligned} \quad (16)$$

$$\mathbf{F} = - \int_{-\frac{h}{2}}^{\frac{h}{2}} \mathbf{r}_s^T \mathbf{f} dz$$

$$\bar{\mathbf{S}} = - \int_{\partial\Omega_s} \mathbf{r}_{\sigma}^T \mathbf{E}_3^T \bar{\mathbf{s}} d\Omega_s$$

Applying Integration by parts from fifth and sixth terms in Eq. (15), one can obtain Eqs. (17) and (18).

$$\begin{aligned} \int_A \delta \hat{\boldsymbol{\sigma}}^T \mathbf{G}_{\sigma s}^x \hat{\mathbf{s}} dA &= \int_0^b \int_0^a \delta \hat{\boldsymbol{\sigma}}^T \mathbf{G}_{\sigma s}^x \hat{\mathbf{s}} dx dy \\ &= \int_0^b \delta \hat{\boldsymbol{\sigma}}^T \mathbf{G}_{\sigma s}^x \hat{\mathbf{s}} dy \Big|_{x=0}^{x=a} \end{aligned}$$

$$\begin{aligned}
& - \int_0^b \int_0^a \delta \hat{\boldsymbol{\sigma}}^T \mathbf{G}_{\sigma_s}^x \hat{\mathbf{s}}_{,x} dx dy \\
& = \int_0^b \delta \hat{\boldsymbol{\sigma}}^T \mathbf{G}_{\sigma_s}^x \hat{\mathbf{s}} dy \Big|_{x=0}^{x=a} \\
& - \int_A \delta \hat{\boldsymbol{\sigma}}^T \mathbf{G}_{\sigma_s}^x \hat{\mathbf{s}}_{,x} dA \quad (17) \\
& \int_A \delta \hat{\boldsymbol{\sigma}}^T_{,y} \mathbf{G}_{\sigma_s}^y \hat{\mathbf{s}} dA = \int_0^a \int_0^b \delta \hat{\boldsymbol{\sigma}}^T_{,y} \mathbf{G}_{\sigma_s}^y \hat{\mathbf{s}} dy dx \\
& = \int_0^a \delta \hat{\boldsymbol{\sigma}}^T \mathbf{G}_{\sigma_s}^y \hat{\mathbf{s}} dx \Big|_{y=0}^{y=b} \\
& - \int_0^a \int_0^b \delta \hat{\boldsymbol{\sigma}}^T \mathbf{G}_{\sigma_s}^y \hat{\mathbf{s}}_{,y} dy dx \\
& = \int_0^a \delta \hat{\boldsymbol{\sigma}}^T \mathbf{G}_{\sigma_s}^y \hat{\mathbf{s}} dx \Big|_{y=0}^{y=b} \\
& - \int_A \delta \hat{\boldsymbol{\sigma}}^T \mathbf{G}_{\sigma_s}^y \hat{\mathbf{s}}_{,y} dA \quad (18)
\end{aligned}$$

By substituting of Eqs. (17) and (18) into Eq. (15), the following equation can be obtained:

$$\begin{aligned}
& \int_A [\delta \hat{\mathbf{s}}^T \mathbf{H}_{s\sigma} \hat{\boldsymbol{\sigma}} + \delta \hat{\mathbf{s}}^T \mathbf{G}_{s\sigma}^x \hat{\boldsymbol{\sigma}}_{,x} + \delta \hat{\mathbf{s}}^T \mathbf{G}_{s\sigma}^y \hat{\boldsymbol{\sigma}}_{,y} \\
& + \delta \hat{\boldsymbol{\sigma}}^T \mathbf{H}_{\sigma s} \hat{\mathbf{s}} - \delta \hat{\boldsymbol{\sigma}}^T \mathbf{G}_{\sigma s}^x \hat{\mathbf{s}}_{,x} - \delta \hat{\boldsymbol{\sigma}}^T \mathbf{G}_{\sigma s}^y \hat{\mathbf{s}}_{,y} \\
& + \delta \hat{\boldsymbol{\sigma}}^T \mathbf{H}_{\sigma\sigma} \hat{\boldsymbol{\sigma}} - \delta \hat{\mathbf{s}}^T \mathbf{F}] dA + \delta \hat{\boldsymbol{\sigma}}^T \bar{\mathbf{S}} \\
& + \int_a^b \delta \hat{\boldsymbol{\sigma}}^T \mathbf{G}_{\sigma_s}^x \hat{\mathbf{s}} dy \Big|_{x=0}^{x=a} \\
& + \int_0^a \delta \hat{\boldsymbol{\sigma}}^T \mathbf{G}_{\sigma_s}^y \hat{\mathbf{s}} dx \Big|_{y=0}^{y=b} = 0 \quad (19)
\end{aligned}$$

Eq. (19) can be rewritten as Eq. (20) by rearranging the unknowns in a vector as follows:

$$\begin{aligned}
& \int_A [\delta \hat{\mathbf{s}}^T \quad \delta \hat{\boldsymbol{\sigma}}^T] \left(\mathbf{G} \begin{Bmatrix} \hat{\mathbf{s}}_{,x} \\ \hat{\mathbf{s}}_{,y} \\ \hat{\boldsymbol{\sigma}}_{,x} \\ \hat{\boldsymbol{\sigma}}_{,y} \end{Bmatrix} + \mathbf{H} \begin{Bmatrix} \hat{\mathbf{s}} \\ \hat{\boldsymbol{\sigma}} \end{Bmatrix} - \begin{Bmatrix} \mathbf{F} \\ \mathbf{0} \end{Bmatrix} \right) dA \\
& + \delta \hat{\boldsymbol{\sigma}}^T \bar{\mathbf{S}} + \int_0^b \delta \hat{\boldsymbol{\sigma}}^T \mathbf{G}_{\sigma_s}^x \hat{\mathbf{s}} dy \Big|_{x=0}^{x=a} \\
& + \int_0^a \delta \hat{\boldsymbol{\sigma}}^T \mathbf{G}_{\sigma_s}^y \hat{\mathbf{s}} dx \Big|_{y=0}^{y=b} = 0 \quad (20)
\end{aligned}$$

where \mathbf{H} and \mathbf{G} are

$$\begin{aligned}
\mathbf{H} & = \begin{bmatrix} \mathbf{0} & \mathbf{H}_{s\sigma} \\ \mathbf{H}_{\sigma s} & \mathbf{H}_{\sigma\sigma} \end{bmatrix} \\
\mathbf{G} & = \begin{bmatrix} \mathbf{0} & \mathbf{0} & \mathbf{G}_{s\sigma}^x & \mathbf{G}_{s\sigma}^y \\ -\mathbf{G}_{\sigma s}^x & \mathbf{G}_{\sigma s}^y & \mathbf{0} & \mathbf{0} \end{bmatrix} \quad (21)
\end{aligned}$$

Since Eq. (20) must satisfy all virtual fields, the system of partial differential Eq. (22) must be satisfied.

$$\mathbf{G} \begin{Bmatrix} \hat{\mathbf{s}}_{,x} \\ \hat{\mathbf{s}}_{,y} \\ \hat{\boldsymbol{\sigma}}_{,x} \\ \hat{\boldsymbol{\sigma}}_{,y} \end{Bmatrix} + \mathbf{H} \begin{Bmatrix} \hat{\mathbf{s}} \\ \hat{\boldsymbol{\sigma}} \end{Bmatrix} = \begin{Bmatrix} \mathbf{F} \\ \mathbf{0} \end{Bmatrix} \quad (22)$$

The above system of partial differential Eq. (22) is the governing equations of plate. By choosing appropriate section shape functions for displacement and stress field, accurate solution can be obtained.

3. Simply Supported Plate

In this section the above formulation is examined by considering a simply supported boundary condition plate subjected to uniform and sinusoidal load. To ensure that the model is well-posed, the following equation is required to be satisfied [20]:

$$\nabla \cdot \boldsymbol{\sigma} = \mathbf{s} \quad (23)$$

In addition, it is assumed that the shape function r consists of polynomial terms with their special degree. Consequently, to satisfy Eq. (23), the following degrees for stress and displacement field are considered:

$$\deg(r_{\sigma_x}) = \deg(r_{\tau_{xy}}) = \deg(r_{\tau_{xz}}) - 1 = \deg(r_u)$$

$$\deg(r_{\tau_{xy}}) = \deg(r_{\sigma_y}) = \deg(r_{\tau_{yz}}) - 1 = \deg(r_v) \quad (24)$$

$$\deg(r_{\tau_{xz}}) = \deg(r_{\tau_{yz}}) = \deg(r_{\sigma_z}) - 1 = \deg(r_w)$$

where \deg . indicates the considered polynomial degree in thickness direction. By choosing quadratic form (degree of 2) for $r_{\tau_{xz}}$, instead of shear correction factor, and considering relations (24), the involved fields in Table 1 are selected.

By using Eq. (16) and then Eq. (21), coefficients of governing equations (22) will be determined.

For simply supported boundary condition, the following Fourier series are considered:

Table 1

Polynomials degrees of profile vectors, continuity properties, and degree of freedom.

Parameter	r_u	r_v	r_w	r_{σ_x}	r_{σ_y}	r_{σ_z}	$r_{\tau_{xy}}$	$r_{\tau_{xz}}$	$r_{\tau_{yz}}$
Degree	1	1	2	1	1	3	1	2	2
Continuity	C^{-1}	C^{-1}	C^{-1}	C^{-1}	C^{-1}	C^0	C^{-1}	C^0	C^0

$$\begin{aligned}
u &= \sum_{m=1}^{\infty} \sum_{n=1}^{\infty} U_{mn} \cos\left(\frac{n\pi x}{a}\right) \sin\left(\frac{m\pi y}{b}\right) \\
v &= \sum_{m=1}^{\infty} \sum_{n=1}^{\infty} V_{mn} \sin\left(\frac{n\pi x}{a}\right) \cos\left(\frac{m\pi y}{b}\right) \\
w &= \sum_{m=1}^{\infty} \sum_{n=1}^{\infty} W_{mn} \sin\left(\frac{n\pi x}{a}\right) \sin\left(\frac{m\pi y}{b}\right)
\end{aligned} \tag{25}$$

In the current method, the stress field is independent of displacement field. According to elasticity theory and considering the above displacement field, the stress field is obtained as follows

$$\begin{aligned}
\sigma_i &= \sum_{n=1}^{\infty} \sum_{m=1}^{\infty} S_{mn}^i \cos\left(\frac{m\pi x}{a}\right) \sin\left(\frac{n\pi y}{b}\right) \quad i = x, y, z \\
\sigma_{xy} &= \sum_{n=1}^{\infty} \sum_{m=1}^{\infty} S_{mn}^{xy} \cos\left(\frac{m\pi x}{a}\right) \cos\left(\frac{n\pi y}{b}\right) \\
\sigma_{xz} &= \sum_{n=1}^{\infty} \sum_{m=1}^{\infty} S_{mn}^{xz} \cos\left(\frac{m\pi x}{a}\right) \sin\left(\frac{n\pi y}{b}\right) \\
\sigma_{yz} &= \sum_{n=1}^{\infty} \sum_{m=1}^{\infty} S_{mn}^{yz} \sin\left(\frac{m\pi x}{a}\right) \cos\left(\frac{n\pi y}{b}\right)
\end{aligned} \tag{26}$$

By substituting Eq. (25) and Eq. (26) into Eq. (22), three algebraic equations are obtained. The unknown coefficients can be solved easily.

4. Numerical Results

In this section, the comparison between previous theories and current work is presented. Eq. (27) shows the dimensionless transversal displacement at the center of the plate for the sinusoidal and uniform load.

$$\bar{w} = \frac{Eh^3}{q_0 a^4} w \times 10^2 \tag{27}$$

The dimensionless transverse displacement for the center of orthotropic plate is shown in Table 2. $K_s = 5/6$ is used as shear correction factor for FSDT. Both square and rectangular plates subjected to both uniform and

sinusoidal loads are considered in this table. The material properties of graphite fabric-carbon matrix layers, which are characterized as orthotropic, is presented in Eq. (28).

$$\begin{aligned}
E_1 &= 25.1 \text{msi}, \quad E_2 = 4.8 \text{msi}, \quad E_3 = 0.75 \text{msi} \\
G_{12} &= 1.36 \text{msi}, \quad G_{13} = 1.2 \text{msi}, \quad G_{23} = 0.47 \text{msi} \\
\nu_{12} &= 0.036, \quad \nu_{13} = 0.25, \quad \nu_{23} = 0.171
\end{aligned} \tag{28}$$

As illustrated in Table 2, there is a very little difference between the current work and exact elasticity theory for all different loadings and aspect ratios. Although, there is the same polynomial degree for in-plane displacements in FSDT and the current work, more accurate results are obtained without using shearing correction factor of the current work. There is a small error between all theories with elasticity in thin plates but there was an obligation to choose more complicated theories for thick plates.

Due to applying shear correction factor for FSDT, there isn't notable difference between the current work and FSDT for displacements. On the other hand, FSDT cannot provide correct results for stress, especially for thick plates. In the case of thin plates, the results are very close because the polynomial variations are not prominent. The presented results are in very good agreement compared with elasticity theory. For square thin plate, the obtained results provide exact five-digit accuracy under uniform load. For moderately thick plates more accurate results are obtained, compared with FSDT, because of considering correct variation for shear stress but for rectangular plates its accuracy depends to a/b ratio.

Out-of-plane shear stresses along the thickness for orthotropic plate are shown in Fig. 2. In this figure, τ_{xz} and τ_{yz} are plotted at $(x, y) = \left(0, \frac{b}{2}\right)$ and $(x, y) = \left(\frac{a}{2}, 0\right)$. It is evident that there is a very little difference between the current method and elasticity solution. The dimensionless stress for one layer orthotropic square plate under uniform load is shown in Table 3. The dimensionless ratios are as

$$\begin{aligned}
(\bar{\sigma}_{xx}, \bar{\sigma}_{yy}, \bar{\sigma}_{xy}) &= \frac{\left(\sigma_{xx}\left(\frac{a}{2}, \frac{b}{2}, \frac{h}{2}\right), \sigma_{yy}\left(\frac{a}{2}, \frac{b}{2}, \frac{h}{2}\right), \sigma_{xy}\left(0, 0, -\frac{h}{2}\right)\right)}{q_0 \left(\frac{a}{h}\right)} \\
(\bar{\sigma}_{xz}, \bar{\sigma}_{yz}) &= \frac{\left(\sigma_{xz}\left(0, \frac{b}{2}, 0\right), \sigma_{yz}\left(\frac{a}{2}, 0, 0\right)\right)}{q_0 \left(\frac{a}{h}\right)}
\end{aligned} \tag{29}$$

Table 2
Transverse displacement for the center of orthotropic plate.

	Load	Uniform load					Sinusoidal load				
		a/h	5	10	20	50	100	5	10	20	50
Square	CPT	2.9783	2.9783	2.9783	2.9783	2.9783	1.8870	1.8870	1.8870	1.8870	1.8870
	FSDT	4.7753	3.3878	3.0169	2.9109	2.8956	3.0926	2.1631	1.9160	1.8455	1.8354
	Current	4.7773	3.3899	3.0189	2.9128	2.8976	3.0934	2.1645	1.9173	1.8468	1.8367
	Elasticity	4.7542	3.3872	3.0185	2.9128	2.8976	3.0742	2.1624	1.9170	1.8467	1.8366
Rec.	CPT	2.9772	2.9772	2.9772	2.9772	2.9772	2.3308	2.3308	2.3308	2.3308	2.3308
	FSDT	5.4474	3.5934	3.1348	3.0068	2.9885	4.2330	2.8003	2.4411	2.3404	2.3260
	Current	5.4481	3.5944	3.1357	3.0077	2.9894	4.2331	2.8011	2.4419	2.3412	2.3269
	Elasticity	5.4185	3.5913	3.1351	3.0074	2.9892	4.2080	2.7988	2.4416	2.3412	2.3268

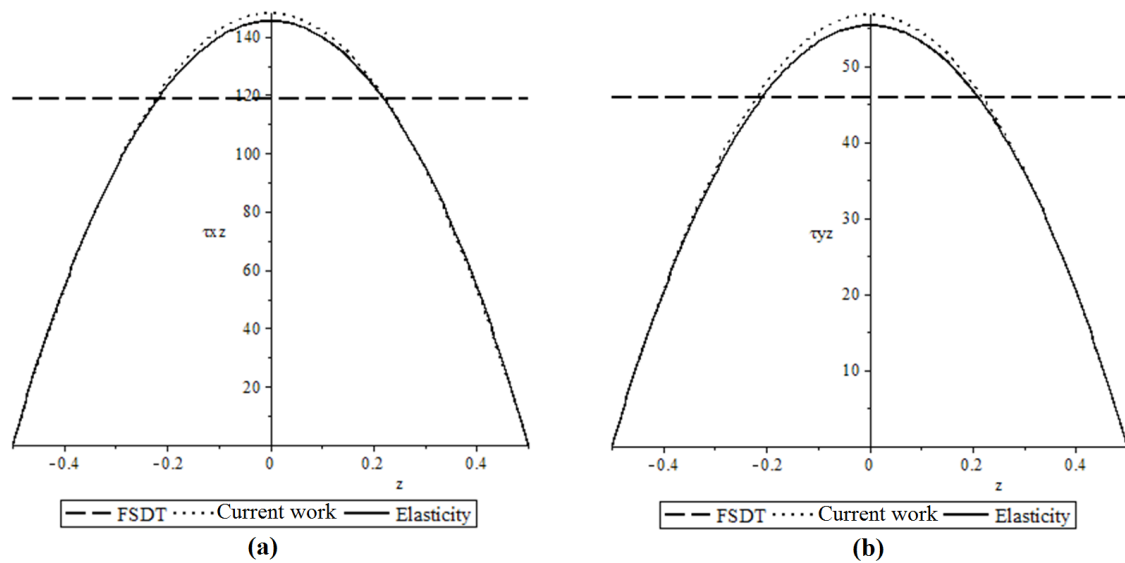


Fig. 2. Out-of-plane shear stresses along thickness for orthotropic plate.

Table 3
Dimensionless stresses for orthotropic square plate under uniform load.

a/h	Theory	$\bar{\sigma}_{xx}$	$\bar{\sigma}_{yy}$	$\bar{\sigma}_{xy}$	$\bar{\sigma}_{xz}$	$\bar{\sigma}_{yz}$
5	FSDT	0.6553	0.1902	0.0409	0.5553	0.2627
	Current	0.6554	0.1901	0.0408	0.6919	0.3260
	Elasticity	0.7270	0.1909	0.0430	0.6331	0.2985
10	FSDT	0.7088	0.1457	0.0356	0.5853	0.2365
	Current	0.7089	0.1456	0.0356	0.7295	0.2932
	Elasticity	0.7283	0.1455	0.0364	0.7014	0.2806
20	FSDT	0.7257	0.1315	0.0336	0.5940	0.2292
	Current	0.7259	0.1314	0.0336	0.7404	0.2841
	Elasticity	0.7308	0.1314	0.0339	0.7263	0.2767
50	FSDT	0.7308	0.1273	0.0330	0.5966	0.2273
	Current	0.7309	0.1271	0.0329	0.7436	0.2816
	Elasticity	0.7317	0.1271	0.0330	0.7362	0.2760
100	FSDT	0.7315	0.1266	0.0328	0.5970	0.2270
	Current	0.7317	0.1265	0.0329	0.7441	0.2812
	Elasticity	0.7318	0.1264	0.0328	0.7380	0.2759

It is worthy to mention that in Table 3, in the current method, the displacement field is independent of stress field. Furthermore, the simplest degree for polynomials is considered for stresses. The FSDT and current work lead to the same results for in-plane stresses, but for out-of-plane stresses, more errors can be seen in FSDT because of constant shear assumption along the thickness. According to Table 3, by increasing the

aspect ratio (thin plates), the difference between different theories becomes smaller. In fact, for thin plate, the effect of transversal shear strains in the thickness direction is small. However, the obtained distribution of shearing stress in the thickness direction is more accurate in comparison with FSDT. Furthermore, there is a small error between the current work and FSDT for in-plane stress for thick plate because the same distribution fields were considered for both theories.

In Table 4, the transverse displacements are presented for two-layer (0/90) composite plates. The material properties are [18]:

$$\begin{aligned} E_1 &= 25E_2, \quad E_2 = E_3, \quad G_{12} = G_{13} = 0.5E_2, \\ G_{23} &= 0.2E_2, \quad \nu_{12} = \nu_{13} = \nu_{23} = 0.25 \end{aligned} \quad (30)$$

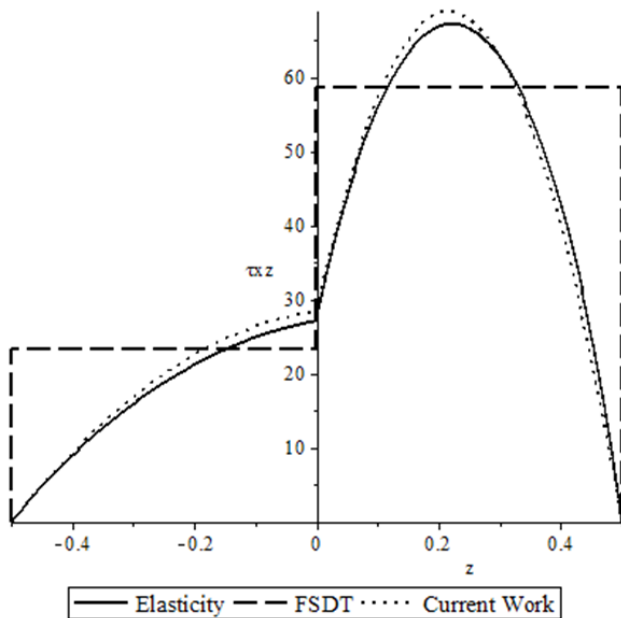


Fig. 3. Shear stress distribution in xz plane for 2 layers of orthotropic plate along thickness.

CPT has the largest error due to its simplification assumptions. The out-of-plane shear stresses for 2 layers are shown in Fig. 3 and Fig. 4.

The current work was compared with finite element method by commercial software Abaqus 6.14. The finite element (FE) modeling of 3-layer (0/90/0) composite plate is shown in Fig. 5(a-b). The plate was square with aspect ratio of $a/h = 5$. Simply support boundary condition with uniform loading was adopted

for plate. In Fig. 5c, the displacement contour is presented. Displacement contour is plotted in Fig. 5d based on the current method by using Maple code. As one can see, there is just 1.5% difference between finite element modeling and the current work. It is noted that by using shell model, FE method could not provide shearing stress in thickness direction.

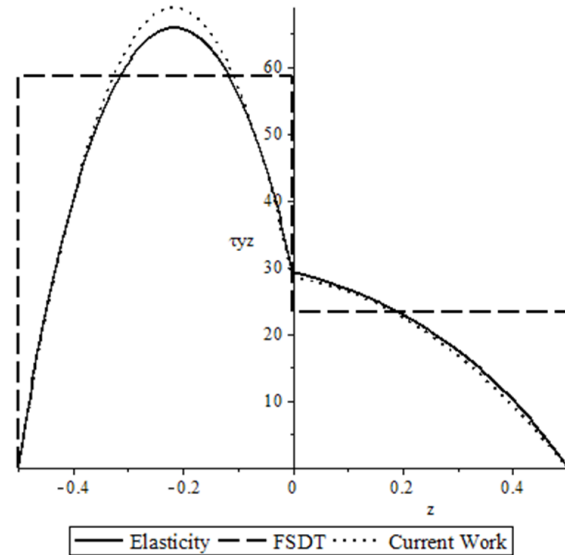


Fig. 4. Shear stress distribution in yz plane for 2 layers of orthotropic plate along thickness.

5. Conclusions

A combined modeling approach based on Hellinger-Reissner Principle and dimension reduction approach was investigated in this paper. First, the dimension of problem was reduced by using combination of cross-section shape functions which were weighted with arbitrary coefficient functions. Then, by applying mixed principle, the partial system of governing equations were obtained. The accuracy and exactness of this method was examined by comparison with FSDT and elasticity theories and FE methods. The substantial benefits of this approach are:

- The proposed approach does not need the use of shear correction factor.
- The current method can provide a very accurate, yet fast and simple solution by increasing the degree of functions in thickness direction.

Table 4

Transverse displacements for 2 layer orthotropic plate.

Theory	5	10	20	50	100
CPT	2.0439	2.0439	2.0439	2.0439	2.0439
FSDT	2.8570	2.1006	1.9119	1.8592	1.8516
Current work	2.8733	2.1451	1.9630	1.9121	1.9048
Elasticity	2.8362	2.1370	1.9611	1.9118	1.9047

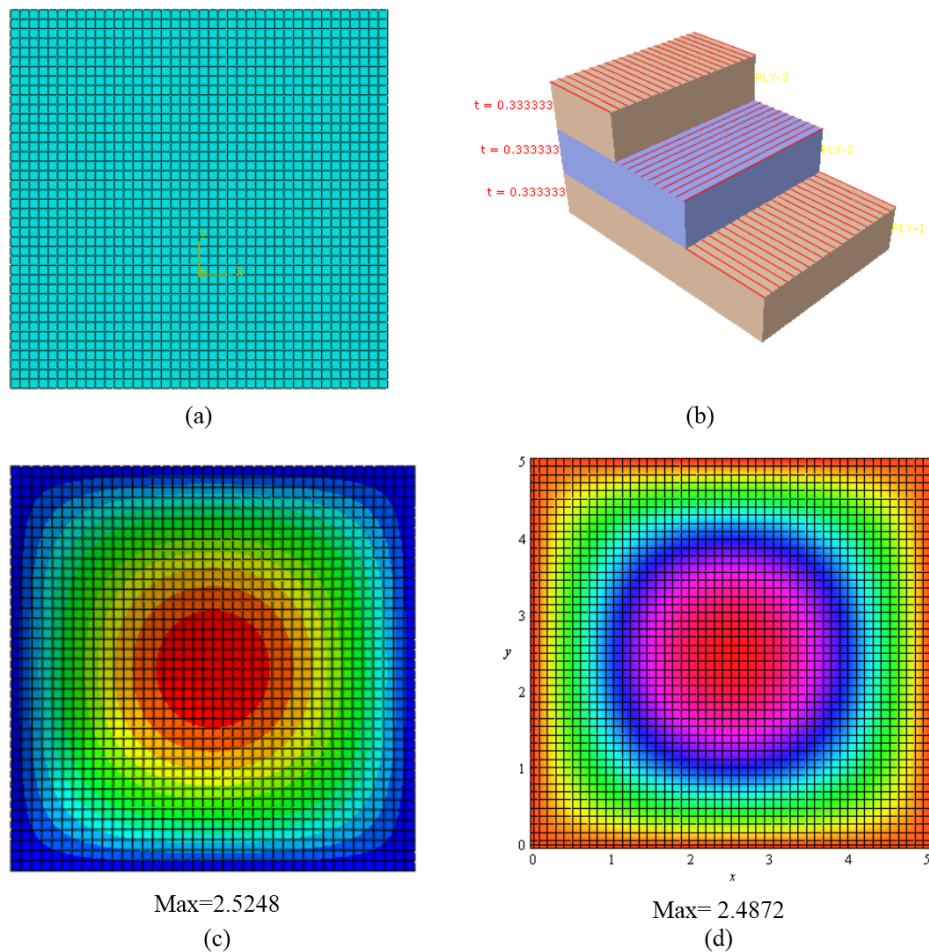


Fig. 5. a) Finite element model, b) Composite plate with 3 plies 0/90/0, c) Vertical displacement distribution from Abaqus, d) Vertical displacement distribution from current work.

- Stress field and displacement field are independent and the stress field can be obtained without computing the displacement field; thus there is no need to post-processing operation for stress field.
- By using current mixed theory, the obtained stress field has more accurate result compared to same displacement description used by other theories.
- The presented method is very convenient for layered composite plates and leads to very accurate results in this category.
- The presented theory can be used for more complex situations like inhomogeneous and thick plates.

References

- [1] R. Khandan, S. Noroozi, P. Sewell, J. Vinney, The development of laminated composite plate theories: a review, *J. Mater. Sci.*, 47(16) (2012) 5901-5910.
- [2] J.N. Reddy, J. Kim, A nonlinear modified couple stress-based third-order theory of functionally graded plates, *Compos. Struct.*, 94(3) (2012) 1128-1143.
- [3] N.J. Pagano, Exact solutions for rectangular bidirectional composites and sandwich plates, *J. Compos. Mater.*, 4(1) (1970) 20-34.
- [4] E. Reissner, On a mixed variational theorem and on shear deformable plate theory, *Int. J. Numer. Meth. Eng.*, 23(2) (1986) 193-198.
- [5] S.M. Alessandrini, D.N. Arnold, R.S. Falk, A.L. Madureira, Derivation and justification of plate models by variational methods, *Plates and Shells*, (1999) 1-21.
- [6] W. Chih-Ping, L. Hao-Yuan, The RMVT-and PVD-based finite layer methods for the three-dimensional analysis of multilayered composite and FGM plates, *Compos. Struct.*, 92(10) (2010) 2476-2496.
- [7] C.P. Wu, H.Y. Li, An RMVT-based third-order shear deformation theory of multilayered func-

- tionally graded material plates, *Compos. Struct.*, 92(10) (2010) 2591-2605.
- [8] E. Carrera, An assessment of mixed and classical theories on global and local response of multilayered orthotropic plates, *Compos. Struct.*, 50(2) (2000) 183-198.
- [9] L. Demasi, ∞^6 mixed plate theories based on the generalized unified formulation, Part I: Governing equations, *Compos. Struct.*, 87(1) (2009) 1-11.
- [10] L. Demasi, ∞^6 Mixed plate theories based on the generalized unified formulation, Part II: Layerwise theories, *Compos. Struct.*, 87(1) (2009): 12-22.
- [11] L. Demasi, ∞^6 Mixed plate theories based on the generalized unified formulation, Part III: Advanced mixed high order shear deformation theories, *Compos. Struct.*, 87(3) (2009) 183-194.
- [12] L. Demasi, ∞^6 Mixed plate theories based on the generalized unified formulation, Part IV: Zig-zag theories, *Compos. Struct.*, 87(3) (2009) 195-205.
- [13] L. Demasi, ∞^6 Mixed plate theories based on the Generalized Unified Formulation, Part V: Results. *Compos. Struct.*, 88(1) (2009) 1-16.
- [14] M. Vogelius, I. Babuška, On a dimensional reduction method, I. The optimal selection of basis functions, *Math. Comput.*, 37(155) (1981) 31-46.
- [15] K.M. Liu, Dimensional reduction for the plate in elasticity on an unbounded domain, *Math. Comput. Modell.*, 30(5-6) (1999) 1-22.
- [16] F. Auricchio, E. Sacco, A mixed enhanced finite-element for the analysis of laminated composite plates, *Int. J. Numer. Meth. Eng.*, 44(10) (1999) 1481-1504.
- [17] F. Daghia, S. De Miranda, F. Ubertini, E. Viola, A hybrid stress approach for laminated composite plates within the first-order shear deformation theory, *Int. J. Solids Struct.*, 45(6) (2008) 1766-1787.
- [18] F. Moleiro, C.M. Mota Soares, C.A. Mota Soares, J.N. Reddy, A layerwise mixed least-squares finite element model for static analysis of multilayered composite plates, *Comput. Struct.*, 89(19-20) (2011) 1730-1742.
- [19] F. Auricchio, G. Balduzzi, C. Lovadina, A new modeling approach for planar beams: finite-element solutions based on mixed variational derivations, *Int. J. Mater. Struct.*, 5(5) (2010) 771-794.
- [20] F. Auricchio, B. Giuseppe, C. Lovadina, The dimensional reduction modelling approach for 3D beams: Differential equations and finite-element solutions based on Hellinger–Reissner principle, *Int. J. Solids Struct.*, 50(25-26) (2013) 4184-4196.
- [21] M. D’Ottavio, A Sublaminar Generalized Unified Formulation for the analysis of composite structures, *Compos. Struct.*, 142 (2016) 187-199.
- [22] M. Arefi, M. Kiani, A.M. Zenkour, Size-dependent free vibration analysis of a three-layered exponentially graded nano-/micro-plate with piezomagnetic face sheets resting on Pasternak’s foundation via MCST, *J. Sandwich Struct. Mater.*, (2017) doi.org/10.1177/1099636217734279.
- [23] M. Arefi, A.M. Zenkour, Size-dependent electro-elastic analysis of a sandwich microbeam based on higher-order sinusoidal shear deformation theory and strain gradient theory, *Int. J. Solids Struct.*, 29(7) (2018) 1394-1406.
- [24] M.L. Ribeiro, G.F.O. Ferreira, R. De Medeiros, A.J.M. Ferreira, V. Tita, Experimental and numerical dynamic analysis of laminate plates via carrera unified formulation, *Compos. Struct.*, 202 (2018) 1176-1185.
- [25] J.N. Reddy, *Mechanics of Laminated Composite Plates and Shells: Theory and Analysis*, CRC Press, (2004).